Fabrication and Characterisation of Ghanaian Bauxite Red Mud-Clay Composite Bricks for Construction Applications

D. Dodoo-Arhin[*], **D. S Konadu, E. Annan, F. P Buabeng, A. Yaya, B. Agyei-Tuffour**

Department of Materials Science and Engineering, University of Ghana, P. O. Box Lg 77, Legon-Accra, Ghana

Abstract   The behaviour of Ghanaian based bauxite red mud-Tetegbu clay composites have been investigated for their applicability in the ceramic brick construction industry as a means of recycling the bauxite waste. The initial raw samples were characterized by X-ray diffraction (XRD), X-ray Fluorescence spectroscopy (XRF), Fourier transform infrared spectroscopy (FTIR), and thermogravimetric analysis (Tg-DTA). The red mud-clay composites have been formulated as 80%-20%, 70%-30%, 60%-40%, 50%-50% and fired at sintering temperatures of 800℃, 900℃ and 1100℃. Generally, mechanical strengths (modulus of rupture) increased with higher sintering temperature. The results obtained for various characterization analyses such as bulk densities of 1.59 g/cm^3 and 1.51 g/cm^3 compare very well with literature and hold potential in bauxite residue eco-friendly application for low-cost recyclable constructional materials.

Keywords   Red Mud-Clay Bricks, Bauxite Residue, Modulus of Rapture, XRD, Thermal Analysis

1. Introduction

In recent times, the exploration of recycling alternatives for several industrial wastes or by-products has become a common practice. Some few industries however do not adhere to proper environmental regulations well leading to environment pollution. Recycling procedures are usually conducted under the influence of legislation or as a means of eliminating disposal cost and avoiding soil and water pollution. In the building industry, recycling of waste materials is environmentally friendly as these materials can be re-use as starting materials for engineering applications. Many of the industrial waste products however, usually contain substantial amounts of inorganic ingredients, such as silicon, aluminium, calcium and iron oxides [1]

One such industrial waste product is the red mud; the main solid by-product in the production of alumina by alkaline extraction routine from bauxite ore via the Bayer process.

Bauxite consists of about 75% of hydrated alumina (Al_2O_3 $3H_2O$ and Al_2O_3 H_2O). During the treatment of the bauxite ore by the Bayer process (figure 1), it is initially crushed and then mixed with a hot solution of sodium hydroxide, NaOH, at ≈175 ℃ and lime liquor and subjected to attack at high pressure and temperature. This condition makes it possible to convert the hydrated alumina and to obtain sodium aluminate solution (Eq. (1)), while the impurities remain in a solid state.
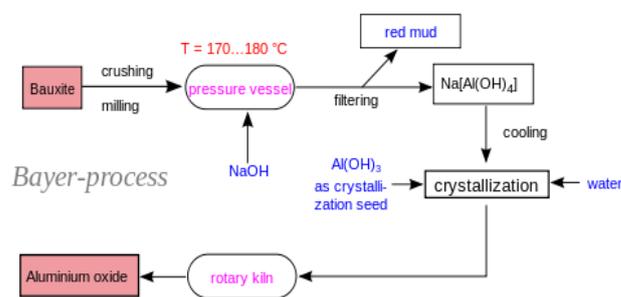
$$Al(OH)_3 + NaOH \rightarrow AlO_2Na + 2H_2O \qquad (1)$$

Figure 1.   The Bayer process for red mud and alumina production

The impurities are separated from the aluminate solution by decantation and filtration, followed by a washing. The solid residues thus obtained are called red mud and are mainly made up of oxides of iron, aluminium, silicon and titanium. However, despite being washed and considered as an inert solid waste, red mud remain strongly alkaline and is highly corrosive. It is usually discharged as highly alkaline slurry (pH 10-13.5) with 15-40 % solids, which is pumped away for appropriate disposal. This strong alkaline character (Na_2O + NaOH = 2.0-20.0 wt.%), restricts the disposal conditions of red mud in order to minimize environmental problems such as soil contamination and ground water pollution. Its chemical and mineralogical composition may however slightly change, depending on the source of bauxite and on the technological processing conditions. It is

* Corresponding author:
ddarhin@yahoo.com (D. Dodoo-Arhin)

composed of six major oxides (Al_2O_3, Fe_2O_3, Na_2O, SiO_2, CaO, and TiO_2), and a large variety of other minor elements.

It is estimated that approximately 35 % - 40 % per ton of bauxite treated ends up as waste via the Bayer process. Furthermore, about 70 million tonnes of bauxite residue or RM are produced yearly worldwide and are not utilised [2]. Africa has 27 % reserves of bauxites deposits and Ghana is known to have one of the high quality bauxites in terms of it turn over in the production of aluminium [3]. The current methods of disposal of the RM in many countries are not safe and hazardous to the ecosystem [4]. The destructive nature of the RM is mainly due to the high alkaline nature having a pH value ranging from 10 to 14 [5]. The seepage of the high pH RM into surface and ground water has adverse consequence on potable water supply to humans, livestock and plants [6-8].

Many researchers have enumerated the various applications of RM and some of them are; special cement preparation, iron powder recovery, clay liners stabilizers, aluminium catalytic usage and construction grade brick [5, 9-12]. The most striking application, in our opinion, was its use in the building industry as bricks. In 1986-1995, the building research in Jamaica, conducted a research to mitigate the effect of adverse effects of RM disposal to the environment. It was successful in stabilizing Bayer processed RM and consequently produced bricks with tremendous bonding strength [13]. In furtherance of this, Annan et al [14], have investigated the physico-mechanical properties of red mud based bricks.

At sintering temperatures of 1000℃ -1100℃, Knight et al.,[15] reported apparent porosity 40-48 %, flexural strength (17.23-27.09) MN/m^2) and compressive strength of 42-83.9MN/m^2. They attributed the high strength and fracture toughness (0.39-0.69) MN/m$^{3/2}$ to glassy state phases in the matrix. Perez et al.,[16] suggested 1100℃ -1200℃ sintering temperatures; attesting better sintering at those temperatures. A 100% bauxite residue ceramic was also sintered at 950℃ by di San Filippo and Usai[17], and achieved compressive strengths comparable to masonry bricks with a shaping pressure of 5000 kg/m^2 and sintering time greater than 48 hours.

Furthermore, Moya et al.,[18] reported that sintering of 100 % bauxite residue ceramics should take place at 1200℃. Using ASTM C373-88 and ASTM C326-82 standard protocols, at a heating rate of 5℃/min and 1000℃ sintering temperature, high sintered body (bulk density 1.7g/cm$_3$) was also produced by Sglavo et al.,[19]. From literature [10-19], sintering temperatures from 950℃ for ceramic bodies results in ceramic piece having high shrinkage and minimum absorbed water, and thus ultimately result in greater mechanical strengths.

It is envisioned that by 2015 processing of Ghanaian bauxite into alumina for the aluminium industry will commence; hence the need for effective recycling methods of the red mud residue instead of disposing it into the environment with all its implications.

The present study investigates the properties of Ghanaian bauxite red mud-clay composite bricks using bauxite and plastic clays from the western (Awaso) and greater Accra (Tetegbu) regions of Ghana respectively. The initial raw materials (bauxite, red mud and clay) have been characterised from x-ray fluorescence spectroscopy (XRF), X-ray diffraction (XRD), Fourier Transform Infrared Spectroscopy (FTIR) and Thermal analysis (Tg/DTA) point of view. Results of the physical and mechanical properties of the Awaso red mud-Tetegbu clay composite brick (ARM-TC) batch formulations sintered at 800℃, 950℃, and 1100℃ are discussed.

2. Experimental

2.1. Materials and Methods

Sample Preparation

The Awaso bauxite sample for the red mud production and Tetegbu clay samples were obtained from the Western and Greater Accra regions of Ghana respectively as shown in figure 2.

In a typical red mud production via the Bayer process, bauxite samples were reduced to fine particle size of ≈100μm by milling using a Thomas ball-mill machine and granulometer. The milled bauxite was digested in a 1000ml Pyrex volumetric flask containing a hot (135℃ - 140 ℃) 2M NaOH solution for about 30minutes under constant stirring to allow even dispersion. The homogenous mixture was then allowed to cool to ambient temperature and the particles allowed to sediment. The liquid phase was then decanted and the residue (red mud) dried in an autoclave at 110℃ for ≈ 48 hours. The samples were then allowed to cool overnight to room temperature.

Characterization of the Bauxite, Clays and Red mud

X-Ray Fluorescence mineralogical composition of the samples was determined using a Thermo Fisher ARL9400 XP+ Sequential XRF equipped with a WinXRF software was for analyses. The samples were milled in a tungsten-carbide milling pot to achieve particle sizes <75micron. The samples were dried at 100℃ and roasted at 1000℃ to determine Loss on Ignition (LOI) values. 1g Sample was mixed with 6g lithium tetraborate flux ($Li_2B_4O_7$) and fused at 1050℃ to make a stable fused glass bead. For trace element analyses the sample was mixed with a PVA binder and pressed into a pellet using a 10 ton press.

X-ray powder diffraction (XRD) patterns were collected on an XPERT-PRO diffractometer (PANalytical BV, Netherlands) with theta/theta geometry, operating a cobalt tube at 35 kV and 50 mA. The goniometer is equipped with automatic divergence Slit and a PW3064 spinner stage. The XRD patterns of all specimens were recorded in the 5.0°- 90° 2θ range with a step size of 0.017° and a counting time of 14 s per step. Qualitative phase analysis was conducted using the X'Pert Highscore plus search match software.

(a)
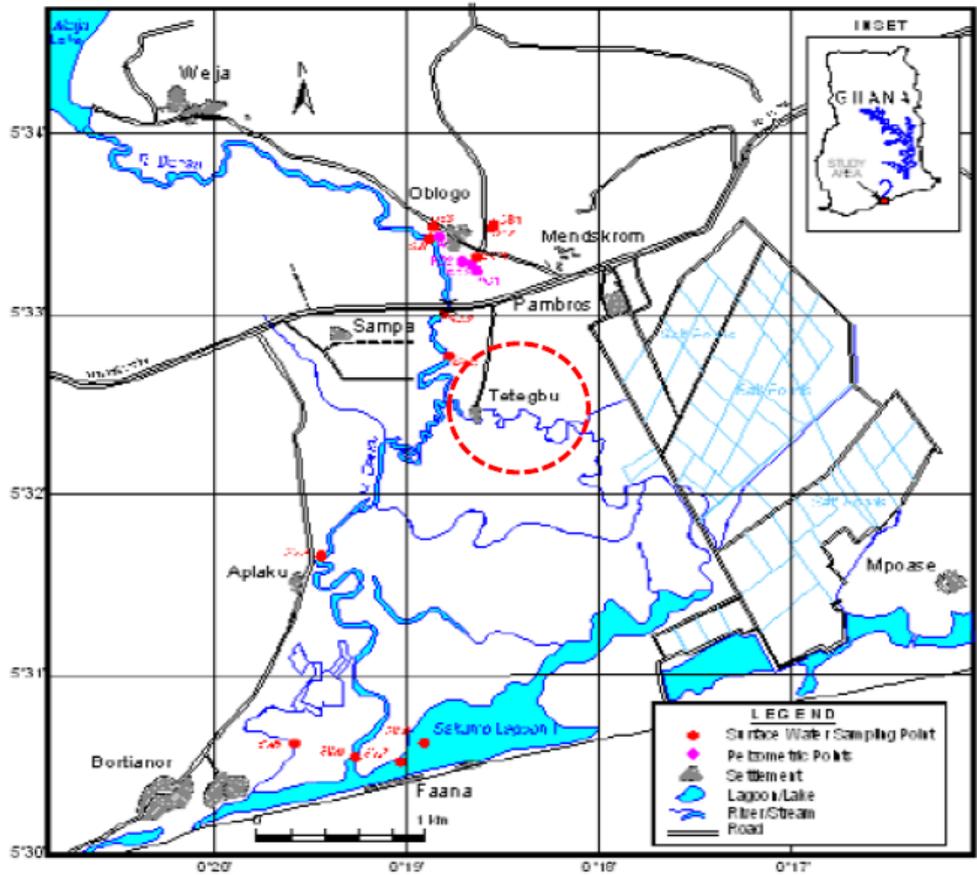
(b)

Figure 2. Geological map of Ghana showing (a) bauxite deposits and (b) Tetegbu clay deposit site (red dash circle)

Transmission FTIR spectra were recorded on a Vertex 70v (Bruker) spectrometer in the 4000-400 cm^{-1} range with 4 cm^{-1} resolution. Sample compartment was evacuated during acquisition and the contact between the sample and the diamond ATR crystal is 2 mm diameter. Spectra were recorded and analysed with the Opus software.

The thermal stability of the various phases in the samples was studied by DTA/TG under air flow of 50 mL/min. The samples were thermally analysed by placing 25mg of the specimens in an alumina (Al_2O_3) crucible (100mg capacity), subjected to a linear heating ramp between 15 ℃ and 1200 ℃ at a rate of 10 ℃/min and a cooling rate of 50 ℃/min, using a standard SDT Q600 (V20.9 Build 20) TG/DTA instrument. The test measurements were made for the mass change (loss) of the sample as a function of the temperature and the phase changes by the adsorption or the emission of energy. A sapphire standard was used to calibrate the thermal response due to heat flow as well as the temperature prior to analysis.

Bauxite Red Mud- Clay Bricks Fabrication

Batch formulations of the bricks fabricated using the Awaso red mud and Tetegbu clay are given in Table-1 with sample batch codes. The Red Mud-Clay composite batches were prepared in a batch mixer of 50:50, 60:40, 70:30 and 80:20 weight percentages respectively under the same condition. The final composite bricks as shown in figure 3, were formed in an oil lubricated wooden mold of dimensions (6 × 3 ×2) cm^3 (for briquettes) and (20 × 1 × 1) cm^3 for Modulus of rapture-MOR bars according to the Ghana Centre for Scientific and Industrial Research standards. For each formulated batch, brick test pieces were fired at temperatures 800 ℃, 950 ℃ and 1100 ℃ at a heating rate of 5 ℃/min for 5 hours.

Table 1. Batch formulation of bricks

Sample Batch code	Awaso Red mud (% Wt)	Tetegbu clay (% Wt)
AT50-50	50.00	50.00
AT60-40	60.00	40.00
AT70-30	70.00	30.00
AT80-20	80.00	20.00

Figure 3. Bauxite Red Mud-Clay briquettes

Physical Property characterization

To determine the magnitude of the range of moisture content over which the ceramic bodies (bauxite/red mud and clay) remains plastic, a plasticity index (PI) test which is the numerical difference between the liquid limit (LL) and the plastic limit (PL) for a particular material (see equation 2) was carried out using an ELLE international Cassagrande device.

$$Plasticity\ Index,\ (PI) = LL\text{-}PL \qquad (2)$$

The water of absorption characterisation was conducted to estimate the final products' (bricks) susceptibility to seepage of water through its pores when immersed in water. The average weight of a fired briquette was measured in air and then re-weighted after being soaked in water for about one hour. The water of absorption (WA) values were obtained in relation to the apparent porosity (AP) and bulk density (BD) as given in equations (3), (4) and (5), respectively.

$$WA(\%) = \frac{S_w - F_w}{F_w} \times 100 \qquad (3)$$

$$AP(\%) = \frac{W_c - W_a}{W_c - W_b} \times 100 \qquad (4)$$

$$BD = \frac{W_a}{W_c - W_b} \qquad (5)$$

Sw is the soaked weight, Fw is the fired weight, W_a is the sample dry weight in air, and W_b is the weight of soaked sample in water, and Wc is the weight of soaked sample measured in air.

ASTM C830-09 and ASTM D6111-09 standard tests were followed in the determination of the porosity and bulk density respectively. Water of absorption data and apparent porosity variation as the content of AC increases are presented and discussed.

2.2. Flexural strength (Modulus of Rapture-MOR)

Using three point bending testing (ASTM C99/C99M-09 standard protocols), the flexural strength of the test bars were determined. Figure-4 represent the test configuration for specimen dimension of (20 x 1 x 1) cm^3 and distance 7.6 cm (between supports), monotonic loading was done at 1.85kg/min till point of fracture. Equation (6) was used in computing flexural strengths and the average values were recorded from two tests. The effect of clay content on the flexural strength values was investigated.
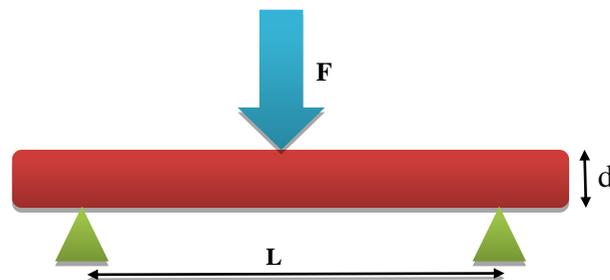

Figure 4. Schematic Three-Point Bending Method

$$\sigma = \frac{3FL}{2dh^2} \tag{6}$$

Where F is load, b is breadth, h is depth, L is distance between supports used.

3. Results and Discussions

3.1. Chemical Analysis (X-Ray Florescence Spectroscopy)

The industrial applications of ceramic materials are greatly influenced by their mineralogical composition as well as their physical and chemical properties[20]. One of the widely used analytical tools in the determination of elemental/chemical composition of ceramic materials is the X-ray fluorescence spectroscopy. The XRF analytical results of the Awaso bauxite, its red mud (RM) and Tetegbu plastic clay are presented in Table-2 which agrees with results obtained by Liu et al.,[12].

Table 2. Major oxides compositions from XRF analysis

Major oxides	Awaso Bauxite (%)	Awaso Red mud (%)	Tetegbu Clay
Al_2O_3	65.15	51.07	15.19
SiO_2	2.75	2.15	68.91
Fe_2O_3	6.99	7.15	3.15
Na_2O	1.05	2.84	0.83
TiO_2	1.93	1.77	1.09
CaO	0.06	1.07	0.85
L.O.I	23.08	33.9	5.63

It is worth stating that the dominant red colour of both the Red Mud and bauxite is attributed to the fairly well dispersed particles of iron oxide (Fe_2O_3) in both samples[1, 21]. The Other oxides found with weight percentages less than 1% are for Awaso bauxite: MgO (0.08%), P_2O_5 (0.15%), SO_3 (0.13%), K_2O (0.04%), MnO (0.01%); for Awaso Red Mud: MgO (0.22%), P_2O_5 (0.15%), SO_3 (0.10%), K_2O (0.04%), and MnO (0.01%). and for Tetegbu clay: MgO (0.48%), P_2O_5 (0.03%), SO_3 (0.01%), K_2O (0.08%), and MnO (0.07%). Minor elements found in all the samples include V, Cr, Co, Ni, Cu, Zn, Ga, As, Y, Ba, and Pb. The presence of Na_2O, K_2O, and CaO enhance the liquid phase sintering by forming low melting eutectic compounds and leading to the sintering process[22, 23]. Their presence also aids in reducing the sintering temperature of the final composite brick by melting at a lower temperature and dissolving other grains such as quartz which melt at high temperatures. This may lead to glassy phases which enhance strength and fracture toughness[13].

3.2. XRD Analysis

The element analysis and phase characterization of clays, bauxite and red mud have been reported by various researchers[24,25] over the years with varying compositions of red mud This compositional difference is known to be dependent on the geographical location of the bauxite from which it was obtained.
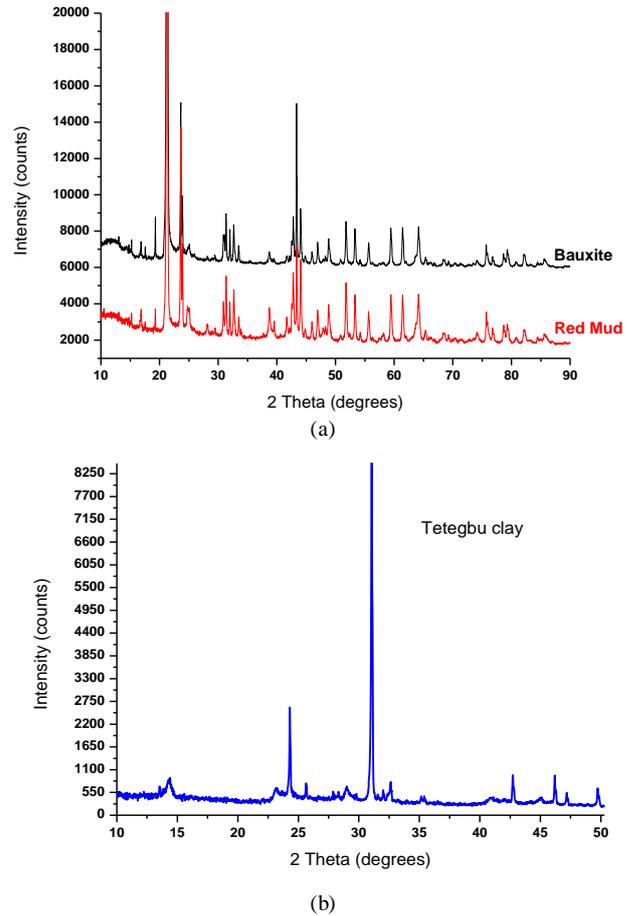

(a)

(b)

Figure 5. XRD pattern of (a) Awaso Bauxite and Red Mud, and (b) Tetegbu Clay

Table 3. Main mineral phases of Awaso red mud

Mineral	Formula	Card no.
Hematite	Fe_2O_3	33-0664
Rutile	TiO_2	21-1276
Perovskite	$CaTiO_3$	22-0153
Quartz	SiO_2,	18-1166
Sodalite	$Na_2O \cdot Al_2O_3 \cdot SiO_2$	16-0612
Boehmite	$AlO(OH)$	21-1307
Goethite	$FeO(OH)$,	26-0792
Gibbsite	$Al(OH)_3$,	33-180
Calcium alumina silicate	$Ca_2Al_2(SiO_4)(OH)_8$,	03-0798

Table 4. Core mineral composition of the Tetegbu clay

Mineral	Formula	Card no.
Quartz	SiO_2,	18-1166
Kaolinite	$Al_2Si_2O_5(OH)_4$	75-0938
Low Albite	$Na(AlSi_3O_8)$	84-0982
Gypsum	$CaSO_4(H_2O)_2$	76-1746
Microline	$KAlSi_3O_8$	84-1455

The XRD pattern for the bauxite, red mud and clay samples are shown figure-5 and supported with XRF analyses in table-2. The main mineral phases identified in the Awaso red mud and the core mineral composition of the

Tetegbu secondary clay samples using the X'pert Highscore qualitative analysis software are shown in tables-3&4 respectively.

3.3. Thermal Analysis (TG-DTA)

The main mineral phases of dried red mud at room temperature are calcite ($CaCO_3$), dicalcium Silicate (Ca_2SiO_4), hematite (Fe_2O_3), perovskite ($CaTiO_3$), gibbsite ($Al(OH)_3$), and CaO. The TG-DTA thermograms (figure 6) show a continuous weight loss distributed in the range of $25–1200°C$. The figure shows two main portions of mass loss as the rise of temperature. The first one is during the heating temperature interval of $50–550°C$ when the physically absorbed water and chemically bound water is off.
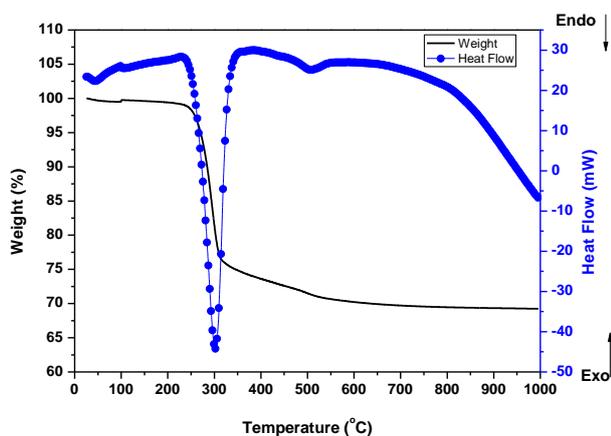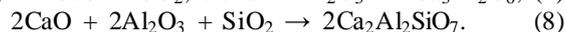
(a)
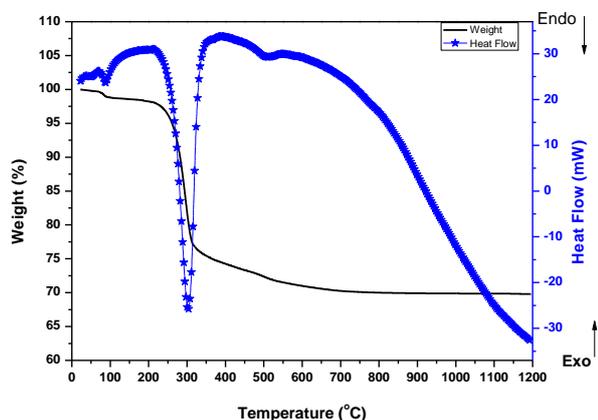
(b)

Figure 6. Tg (Wt%)-DTA (Heat flow) thermographs of (a) Awaso Bauxite, and (b) Awaso Red mud

Before the firing temperature is up to $500°C$, the sample loses $≈8.26\%$ total of its weight. The proportion of physically absorbed water is small. Comparing this result with the results of the XRD analysis, the lost chemically bound water could be mainly attributed to the decomposition of gibbsite ($Al(OH)_3$) to alumina (Al_2O_3) and H_2O which can combine with the CaO to form tricalcium aluminate or Gehlenite.

The more rapid decline in the range of $550–900°C$ with a mass change of $≈21.81\%$ could be attributed to the release of CO_2[25]. The release of CO_2 is due to the decomposition of

Calcite ($CaCO_3$) into CaO. The chemical equations during this phase transformation are as following:

$$CaCO_3 → CaO + CO_2, \quad 3CaO + Al_2O_3 → Ca_3Al_2O_6, \quad (7)$$
$$2CaO + 2Al_2O_3 + SiO_2 → 2Ca_2Al_2SiO_7. \quad (8)$$

The phases of tricalcium aluminate ($Ca_3Al_2O_6$) and gehlenite ($Ca_2Al_2SiO_7$) start to develop in the $800–900°C$ range. There is no obvious mass change or phase change above $900°C$

3.4. FTIR

The molecular structure of red mud has been identified in the infrared region with Infrared Spectroscopy analysis. According to the given IR spectrum in Figure 7, the peak at 3426 cm^{-1} wavelength shows hydroxyl bonds of gibbsite. Free H_2O peaks at 1642.88 and 1454.36 cm^{-1} wavelengths states CaO component in calcite.
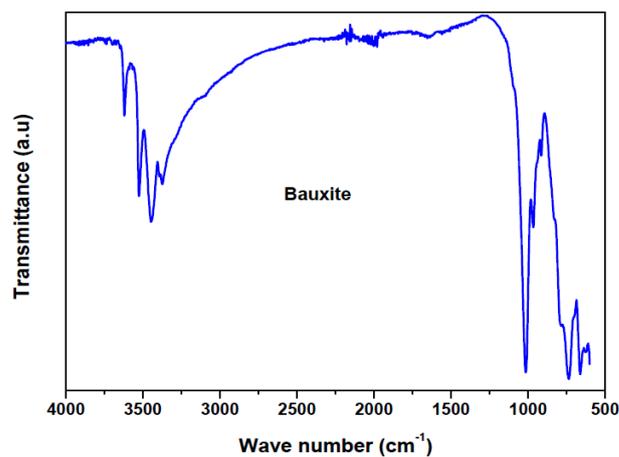
(a)
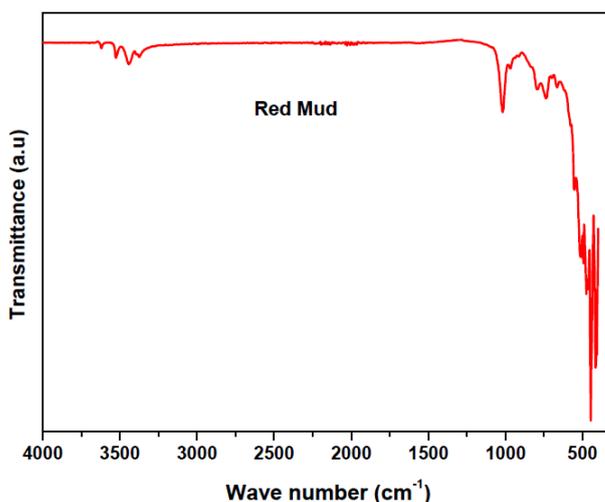
(b)

Figure 7. FTIR of (a) Bauxite and (b) red mud samples

The peaks at 999.3 cm^{-1} wavelength shows Si-O bond, at 874.66, 712.21 and 628.25 cm^{-1} wavelengths show the $Al^{3+}-O^{2-}$ bonds and at 559.40 and 479.01 cm^{-1} wavelengths show $Fe^{3+}-O^{2-}$ bonds.

3.5. Physical and Mechanical Properties

3.5.1. Plasticity Index (PI)

In the building construction industry, determination of the plasticity index is very important, in ensuring that the sample (bricks or blocks) retains the correct amount of shear strength and not too much change in volume as it expands and shrinks at different moisture contents. Hence, the greater the plasticity index, the more plastic, compressible and greater the volume change characteristics of the ceramic samples.

Table 5. Plasticity index for the red mud and Clay

| Sample	Liquid limit (LL)	Plastic limit (PL)	Plasticity Index (PI)
Awaso red mud	29.36	25.24	4.12
Tetegbu clay	48.00	22.57	25.43

The high plasticity index (25.43) of Tetegbu clay as shown in table-5 makes it a good binder which improves significantly the inter-particle cohesion of the Awaso red mud (4.12) in the "green" body formation. This high plasticity exhibited by the clay when mixed with the right proportion of water, as well as the subsequent hardening in the drying and sintering stages of the final test samples could be attributed to the large quantity of phylosilicates in the clay evidenced in the XRF and XRD data.

3.5.2. Water of Absorption, Apparent Porosity, Bulk Density and Flexural Strength (Modulus of Rapture-MOR)

During the firing/sintering of samples, there is a degree of linear shrinkage related to processes of pore formation and densification of the samples which influences the strength of the final test product. Increasing the red mud content tends to increase the bulk density, thereby decreasing their porosity and resulting in expansion of the samples. The presence of red mud leads to the formation of macropores which closes gradually as the quantity of red mud increases. The total porosity of the sintered samples can be open or closed. The porosity of the open-pore samples can be calculated from the results of water of absorption test. A low quantity of open pores is desirable; as it is an indication that the samples can better resist environmental conditions and possesses greater durability. It is worth stating that when there is a high degree of shrinkage of the brick samples, there will be a corresponding increase in the volume of the pores, thus lowering the absorption rate. The high content of the fluxes (see XRF, XRD and FTIR data) generates more vitreous phases which fill in the pores of the samples thereby decreasing the porosity and the quantity of water absorbed.

The water of absorption of a test piece determines the measure of the extent to which the test piece is susceptible to seepage of water through its pores when immersed in water. This test gives an idea on how the brick products produced will behave when used in various applications. Test pieces having higher water of absorption means they are more porous in nature. It could also be observed that, as the clay content reduced, the water of absorption decreased. This could be attributed to the RM quantity in the fired brick and of all the batches. Low water of absorption in the test pieces will have higher strength and durability. Since if the water of absorption is low, it restricts the amount of water may cause deterioration. Water existing in the pores of the products will be cyclically expanded and contracted and this will generate stresses within the material thereby resulting in the weakening of the product.
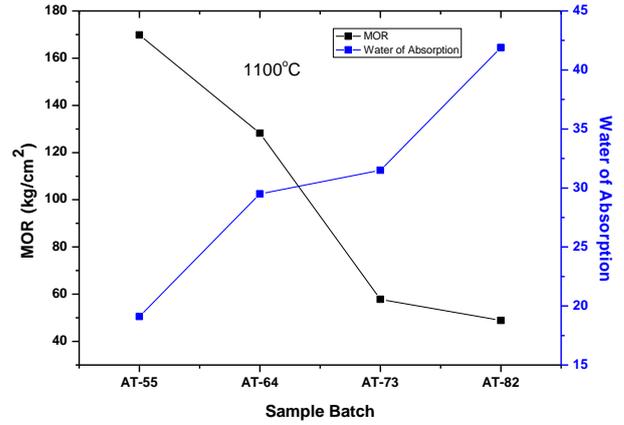
(a)
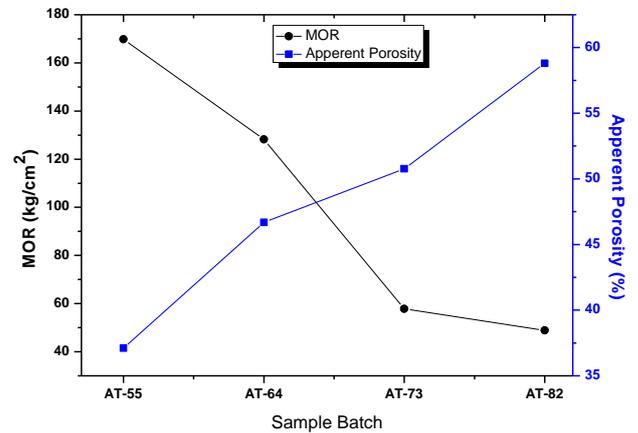
(b)

Figure 8. variation of (a) water of absorption and (b) apparent porosity with modulus of rapture in relation to batch formulation of the composite bricks at 1100 °C

The relationship between the water of absorption and the flexural strength of the batch formulated bricks is shown in figure 8a.

Apparent porosity is the proportion of the bulk volume represented by spaces or pores connecting to each other and with the atmosphere.

With the increase in temperature beyond 1000 °C, most of the pores within the test pieces are expected to be eliminated due to sintering which gives rise to products with less porosity. At a firing temperature of 1100 °C the apparent porosity values increased from 37.1% (AT55) to 58.8% (AT82); at 950 °C, it increased 43.5% (AT55) to 59.4% (AT82); and at 800 °C, it increased from 44.2% (AT55) to 58.5% (AT82). Hence at 50:50, the apparent porosity

decreases with increase in temperature as expected of a sintering phenomenon. However, at ratios of 80:20, the average apparent porosity of about 59% observed could be attributed to the opening up of micro cracks (formation process) at high temperatures. At 1100°C, the flexural strength (MOR) decreases from 169.8kg/cm^2 for AT55 to 48.9kg/cm^2 for AT82.

The general trend of the apparent porosity and the modulus of rapture is shown in figure 8b where an increase in the apparent porosity results in the decrease in the strength (MOR) of the final composite brick samples. A similar trend is observed for the water of absorption.

Bulk density is simply, the mass per unit volume of a dry brick, including the hollow spaces or pores in the brick test pieces. The Bulk density also relates directly to the degree of shrinkage of the samples since as the size of the samples decrease slightly, the weight loss after sintering remains constant in the samples while the volume of the sample decreases (although weight remaining nearly constant) as well as the density of the samples increasing. Bulk density also influences the strength of the bricks, since, as the samples become denser, their lower porosity gives them greater strength. Figures 8a-b illustrates the bulk density variation of the test pieces with temperature.

An increase in bulk density results when the particles are able to pack themselves efficiently in the lattices of the bulk mass. The bulk density of the test pieces increased as the sintering temperature increased. However, TA82 at 950°C firing and TA55 at 1100°C firing deviated from this pattern. This could be attributed to the formation of new phases at those temperatures which were not able to compact themselves very well leading to distortions in the final brick samples. This probably made them decrease in bulk density instead of increasing as the temperature of firing was raised higher.

Averagely, bulk density increased as the binder content increased at 800°C and 950°C and this relationship became highly independent at 1100°C firing. This is phenomenon is attributed to the reduction in the inter-particle distance of the grains as the binder content is increased leading to a well dense body. The bulk densities of TA55 (1.59 g/cm^3) and TA64 (1.51 g/cm^3) agreed with the Indian standards specifications at 800°C firing.

3.5.3. Effect of Clay Content and Sintering Temperature on MOR

Better sintering of the composite brick samples tend to increase with increase in temperature from 800°C and above leading to reduction in the average pore sizes. For the same sintering temperatures, the mechanical strength (modulus of rapture) was observed to increase with increasing composition of the Tetegbu clay as shown in Figure-9. This binder increment minimizes the porosity of the samples by increasing the cohesion forces while decreasing their inter-particles separation[26]. During the sintering process, polymorphic phase transformations occur as a result of

chemical reactions leading into complex compounds at high temperatures.

3.6. Effect of Clay Content and Sintering Temperature on MOR

Better sintering of the composite brick samples tend to increase with increase in temperature from 800°C and above leading to reduction in the average pore sizes. For the same sintering temperatures, the mechanical strength (modulus of rapture) was observed to increase with increasing composition of the Tetegbu clay as shown in Figure-9. This binder increment minimizes the porosity of the samples by increasing the cohesion forces while decreasing their inter-particles separation[26]. During the sintering process, polymorphic phase transformations occur as a result of chemical reactions leading into complex compounds at high temperatures. These tend to aid in the quick sintering process and impacts on the stability of the material due to the decrease or increase in the volume of the system[27, 28].

At temperatures beyond 900°C, the presence of fluxes (K$_2$O, Na$_2$O, Fe$_2$O$_3$, and CaO) in the composite bricks begins to yield glassy phases aligning themselves very well along the grain boundaries of the mixtures to achieve high densification which increase the bulk density and consequently the mechanical strength.
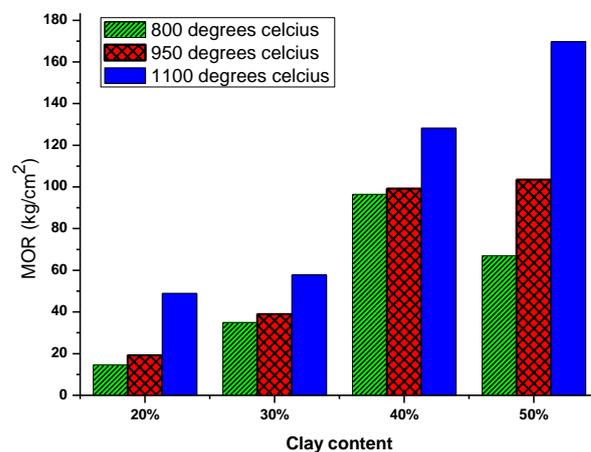

Figure 9. Effect of Clay Content on Flexural Strength (MOR) at different firing temperatures

4. Conclusions

The possibility of using Bayer processed bauxite residue (red mud) as a raw material in brick production for building construction applications has been investigated. Bricks were fabricated from batch mixes of laboratory processed red mud and a highly plastic clay material, obtained locally in varying quantities.

The chemical, physical and mechanical properties have been investigated for varying red mud-clay contents at firing temperatures of 800°C, 950°C, and 1100°C. Sintering at 1100°C produced the brick with the best properties mechanical properties. Physical properties such as apparent

porosity and water of absorption reduced while the mechanical strength (modulus of rupture), and the bulk densities increased at higher sintering temperature.

Considering the physical and mechanical properties of the fabricated brick samples, the batch formulation which contained 50% each of the Awaso red mud and Tetegbu clay is considered the best combination with optimal properties for the construction bricks application. Other batch formulations with 20-30% clay content were also within tolerable limits and could be employed in lighter weight structural applications.

ACKNOWLEDGEMENTS

REFERENCES

[1] P.E. Tsakiridis, S. Agatzini-Leonardou, P. Oustadakis, Red mud addition in the raw meal for the production of Portland cement clinker, Journal of Hazardous Materials B116 (2004) 103-110.

[2] Meseaguer S, Pardo F, Jordan M.M, Sanfeliu T and Gonzalez I. 2010. Ceramic behaviour of five Chilean clays which can be used in Manufacture of ceramic tile bodies. Appl. Clay Sci. 47: 372-377.

[3] Kesse G.O. 1985. The Mineral and Rock Resources of Ghana. ABalkema. Rotterdam Netherlands.

[4] John I. Glanville. 1991. Evaluation Report on Bauxite Bricks. IDRC, Ottawa, IDRC FILE, Canada. 3: 86-1039.)

[5] M. Gräfe, G. Power and C. Klauber. 2011. Bauxite residue issues: III. Alkalinity and associated chemistry, Hydrometallurgy. 108: 60-79.

[6] Pascual J., Corpas F. A., López-Beceiro J., Benfez-Guerrero M. and Artiaga R. 2009. Thermal Characterization of a Spanish Red mud. Journal of Thermal Analysis and Calorimetry. 96(2): 407-412,

[7] Hind A., Bhargava S. and Grocott S. 1999. The surface chemistry of Bayer process solids: a review. Colloids and Surfaces A: Physicochem. Eng. Aspects. 146: 359-374.

[8] Nevin Y. and S. Vahdettin. 2000. Utilization of bauxite waste in ceramic glazes. Ceramics International. 26(5): 485-493.

[9] Cablik V. 2007. Characterization and applications of red mud from Bauxite processing. Gospodarka Surowcami Mineralnymi, tom 23, Zeszyt4.

[10] Sushil Snigdha and Batra V. S. 2008. Catalytic applications of red mud, an aluminium industry waste: A review. Applied Catalysis B, Environmental. 81: 64-77.

[11] Kalkam Ekrem. 2006. Utilization of red mud as a stabilization material for the preparation of clay liners. Engineering Geology. 87: 220-229.

[12] Liu Wancho, Yang Jiakuan and Xiao Bo. 2009. Application of Bayer Red Mud for iron recovery and building material from alumosilicate residues. Journal of Hazardous Materials. 161: 474-478.

[13] Karaman S., Ersahin S. and Gunal H. 2006. Firing temperature and firing time influence on mechanical and physical properties of clay bricks. Journal of scientific and industrial research. 65: 153-159.

[14] E. Annan, B. Agyei-Tuffour, L. N. W. Damoah, D. S. Konadu and B. Mensah. Physico-mechanical properties of bauxite Residue-clay bricks, ARPN Journal of engineering and applied sciences, vol. 7, no. 12, 2012

[15] J.C. Knight, A.S. Wagh and W.A. Reid. 1986. The mechanical properties of ceramics from bauxite waste. J. Mater. Sci. 21(6): 2179-2184.

[16] R.G.A. Perez, R. F. Guitian and S. De Aza Pendas. 1999. Industrial obtaining of ceramic materials from the Bayer process red muds. Bol. Soc. Esp. Ceram. 38(3): 220-226.

[17] P.A. di San Filippo and G. Usai. 1988. The recycling of red mud from the Bayer Process, part 1, production of masonry bricks at a firing temperature of 950 8C, ZI, Ziegelindustrie Int. 41(2-3): 67-74.

[18] J.S. Moya, F.Morales and V.A. Garcia. 1987. Ceramic use of red mud from alumina plants. Bol. Soc. Esp. Ceram. 26(1): 21-29.

[19] V.M. Sglavo, R. Campostrini, S. Maurina, G. Carturan, M. Monagheddu, G. Budroni and G. Cocco. 2000. Bauxite red mud in the ceramic industry. Part 1: thermal behaviour. J. Eur. Ceram. Soc. 20(3): 235-244.

[20] Tudisca V., Casieri C., Demma F, Diaz M, Pinol L, Terenzi C. and De Luca F. 2011. Firing technique characterization of black-slipped pottery in Prasnesete by low field 2D NMR relaxometry. Journal Archaeol. Sci. 38: 352-359.

[21] S. Srikanth, A.K. Ray, A. Bandopadhyay, B. Ravikumar and J. Animesh. 2005. Phase constitution during sintering of red mud and red mud-fly ash mixtures. J. Am. Ceram. Soc. 88(9): 2396-2401.

[22] Y. Pontikes, C. Rathossi, P. Nikolopoulos, G.N. Angelopoulos, D.D. Jayaseelan and W. E. Lee. 2009. Effect of firing temperature and atmosphere on sintering of ceramics made from bayer process bauxite residue. Ceramics International. 35: 401-407.

[23] Mackenzie J.KD, Meinhold R. H., Brown I.W.M. and White G.V. 1996. The formation of mullite from Kaolinite under various reactions atmospheres. J. Eur. Ceramics Soc. 16: 115-119.

[24] V. M. Sglavo, R. Campostrini, S. Maurina et al., "Bauxite "red mud" in the ceramic industry-part 1: thermal behaviour,"Journal of the European Ceramic Society, vol. 20, no. 3, pp. 235-244, 2000.

[25] X. Liu, N. Zhang, H. Sun, J. Zhang, and L. Li, "Structural investigation relating to the cementitious activity of bauxite

residue-red mud," Cement and Concrete Research, vol. 41, no. 8, pp. 847-853, 2011.

[26] Monteiro S.N. and Vieira C.M.F. 2004. Influence of firing temperature on ceramic properties of clays from Campos's dos Goytacazes. Braz. Appl. Clay Sci. 27: 229-234.

[27] I. Johari, S. Said, B. Hisham, A. Bakar, Z. A. Ahmad, "Effect of the Change of Firing Temperature on Microstructure and

Physical Properties of Clay Bricks from Beruas (Malaysia)", Science of Sintering, 42 (2010), pp. 245-254.

[28] S. A. Bernal, R. M. Gutiérrez, A. L. Pedraza, J. L. Provis, E. D. Rodriguez, S. Delvasto, "Effect of binder content on the performance of alkali-activated slag concretes", Cement and Concrete Research 41 (2011), pp 1-8.